JOURNAL OF BACTERIOLOGY, Feb. 1992, p. 935–946
0021-9193/92/030935-12$02.00/0

Vol. 174, No. 3

Characterization of Novel, Phenol-Soluble Polypeptides Which Confer Rigidity to the Sheath of *Methanospirillum hungatei* GP1

G. SOUTHAM AND T. J. BEVERIDGE*

Department of Microbiology, College of Biological Science, University of Guelph, Guelph, Ontario N1G 2W1, Canada

Received 15 August 1991/Accepted 18 November 1991

Treatment of the *Methanospirillum hungatei* GP1 sheath with 90% (wt/vol) phenol resulted in the solubilization of a novel phenol-soluble group of polypeptides. These polypeptides were purified by the removal of insoluble material by ultracentrifugation and represented approximately 19% of the mass of the sheath. The phenol-insoluble material resembled untreated sheath but had lost its rigidity and cylindrical form. Recombination of phenol-soluble and phenol-insoluble fractions by dialysis to remove phenol resulted in cylindrical reassembly products. Although bona fide sheath (complete with the 2.8-nm lattice) was not produced, a role for the phenol-soluble polypeptides in the maintenance of sheath rigidity is implied. The phenol-soluble polypeptides have limited surface exposure as detected by antibodies on intact sheath; therefore, they are not responsible for the 2.8-nm repeat occurring on the outer face of the sheath. However, longitudinal and transverse linear labeling by protein A-colloidal gold on the outer and inner faces, respectively, occurred with monoclonal antibodies specific to the phenol-soluble polypeptides. Restricted surface exposure of phenol-soluble polypeptides on the sheath highlighted molecular defects in sheath architecture. These lattice faults may indicate sites of sheath growth to accommodate cell growth or division (longitudinal immunogold label) and filament division (transverse immunogold label). The identification of a second group of polypeptides within the infrastructure of the sheath suggests that the sheath is a trilaminar structure in which phenol-soluble polypeptides are sandwiched between sodium dodecyl sulfate–β-mercaptoethanol–EDTA-soluble polypeptides (G. Southam and T. J. Beveridge, J. Bacteriol. 173:6213–6222, 1991) (phenol-insoluble material).

Bacterial surface arrays (S layers) are paracrystalline proteinaceous or glycoproteinaceous assemblies which represent the outermost cell surface feature of many eubacteria and archaeobacteria (19). Disassembly of these S layers typically involves the modification of ionic conditions, hydrogen bonding, and hydrophillic-hydrophobic interactions (12). Solubilization by these modifications supports the concept that covalent linkages are not involved in subunit-subunit bonding.

Methanospirillum hungatei possesses an unusual proteinaceous sheath as its external surface. Unlike most S layers, the sheath does not completely enclose individual cells but is a hollow tube which surrounds both individual cells and chains of two or more cells in concert with multilayered cell spacers and end-plugs (2, 18). The sheath is structurally unique, possessing a 2.8-nm paracrystalline repeat overlying a generally amorphous inner region (5, 24). On the basis of the presence of this 2.8-nm repeat, the sheath is thought to function as a sieve and to exclude molecules larger than acetate (24) or crystal violet (4). For the substrate, this would allow the transfer of the basic nutrients of the bacterium (hydrogen, carbon dioxide, and acetate) into cells and the transfer of its primary metabolic product (methane) out of cells.

Chemical analysis of the sheath has proven difficult (7, 17, 20, 21) owing to its stability in the presence of typical chaotropic and nonionic detergents, denaturants, and digestive enzymes (5). The ability of the sheath to withstand typical dissolution conditions is not consistent with noncovalent intersubunit bonding. In a recent study (20) we used a sodium dodecyl sulfate (SDS)–β-mercaptoethanol (β-ME)–EDTA dissolution procedure to solubilize 74% of the sheath (by mass) as polypeptides which ranged from 10 to 40 kDa. These polypeptides were located on both the inner and outer faces of the sheath. These findings extended the protein bilayer model described by Sprott et al. (21) to a single group of polypeptides distributed in two structurally heterogeneous surfaces (3). Since β-ME was required for good solubilization of the sheath (20, 21), covalent bonding in the form of strategic disulfide bonds (between cysteines) were thought to be responsible for its resilience.

Here we describe a novel group of noncovalently bound polypeptides in the sheath of *M. hungatei* GP1 which are extracted by phenol. These phenol-soluble polypeptides are implicated in the rigidity of the sheath, are integrated into a structural model involving two groups of sheath proteins, and are discussed in reference to sheath growth.

MATERIALS AND METHODS

Bacterial growth conditions. *M. hungatei* GP1 (16) was grown as described by Patel et al. (15).

Purification of sheath. A crude preparation of *M. hungatei* sheath was obtained through spheroplast formation of cell cultures (22) and sucrose gradient centrifugation (23). The crude sheath preparation was reacted with 0.1 M NaOH at room temperature and then with 1% (wt/vol) SDS at 90°C with extensive washing in distilled water (dH_2O) after each treatment (20). The purified sheath was stored at 4°C in dH_2O containing 0.01% (wt/vol) sodium azide. The azide was removed from the sheath by washing via centrifugation (14,000 × *g* for 1 min) prior to further experimentation.

Chemical fractionation of purified sheath. Purified sheath (3 ml of 6.6 mg/ml) was reacted with 90% (wt/vol) aqueous

* Corresponding author.

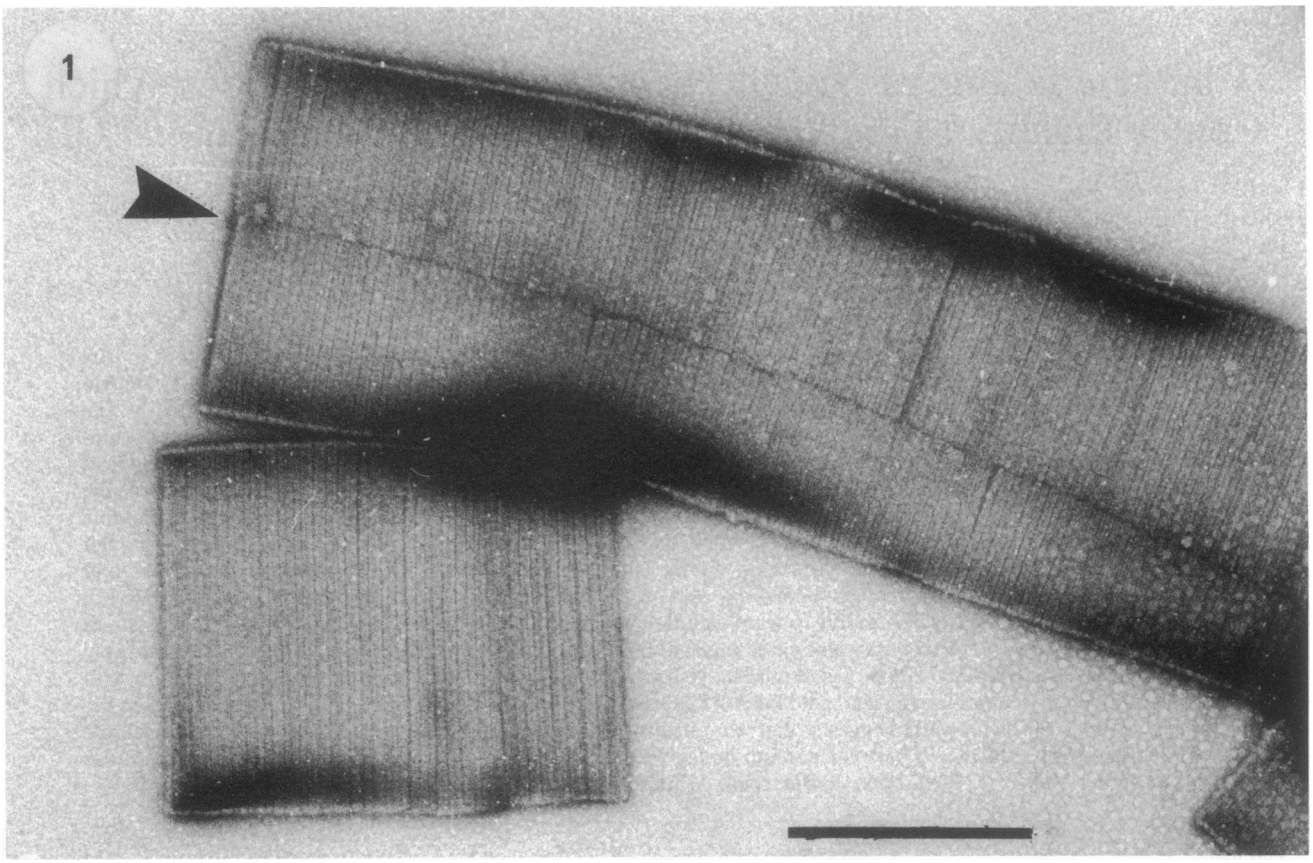

FIG. 1. Negative stain (2% uranyl acetate) of *M. hungatei* GP1 sheath heated in dH_2O at 100°C for 48 h. Note the longitudinal fracture in the sheath tube (arrowhead). Bar, 0.5 μm.

phenol at room temperature for up to 7 days. Routine phenol treatments were carried out at room temperature for 18 h. This reaction mixture was centrifuged at 175,000 × *g* for 1 h at 20°C to pellet insoluble material. The supernatant and the pellet from this centrifugation step were designated as phenol-soluble (PS) and phenol-insoluble (PI) fractions, respectively. These were dialyzed (PS fraction) or resuspended (PI fraction) into either dH_2O or 2% (wt/vol) SDS to remove the phenol prior to further examination. Routine PS and PI preparations involved SDS dialysis at this step. The phenol-treated samples were studied by electron microscopy with negative staining and thin sections of standard embedded material (20) whenever possible. Sheath was also incubated in dH_2O at 100°C for 48 h. The dH_2O-treated sheath was examined by negative staining and electron microscopy.

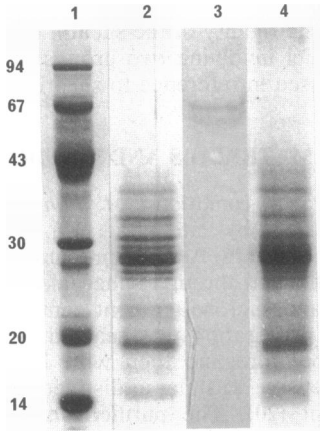

FIG. 2. Coomassie brilliant blue R-250-stained SDS-PAGE gel (15% acrylamide) of sheath which has been treated with various dissolution conditions. Lanes: 1, Bio-Rad low-molecular-weight standard; 2, sheath treated with SDS–β-ME–EDTA for 2 h at 100°C; 3, PS sheath fraction treated with SDS–β-ME–EDTA for 5 min at 100°C; 4, PI fraction treated with SDS–β-ME–EDTA for 2 h at 100°C.

Efficiency of sheath solubilization. To determine the solubilization efficiency of this treatment (same as above), PS and PI fractions (resuspended in 90% [wt/vol] phenol) were placed in preweighed aluminum planchets (Sigma Chemical Co., St. Louis, Mo.) and dried at 110°C until the dry weights were stable. These values were compared with those of an untreated sheath control.

Sheath reassembly. Purified sheath (1 ml; 6.6 mg/ml) was reacted with 90% (wt/vol) phenol for 18 h. The PI fraction was dialyzed against 2% SDS and then washed three times by centrifugation (14,000 × *g*) into dH_2O. The resulting pellet was resuspended in the PS fraction (produced above) and dialysed against 2% SDS. The assembly product of this reaction was examined in thin section by transmission electron microscopy.

Protein determination. Protein concentrations were assayed by using the modified Lowry procedure described by

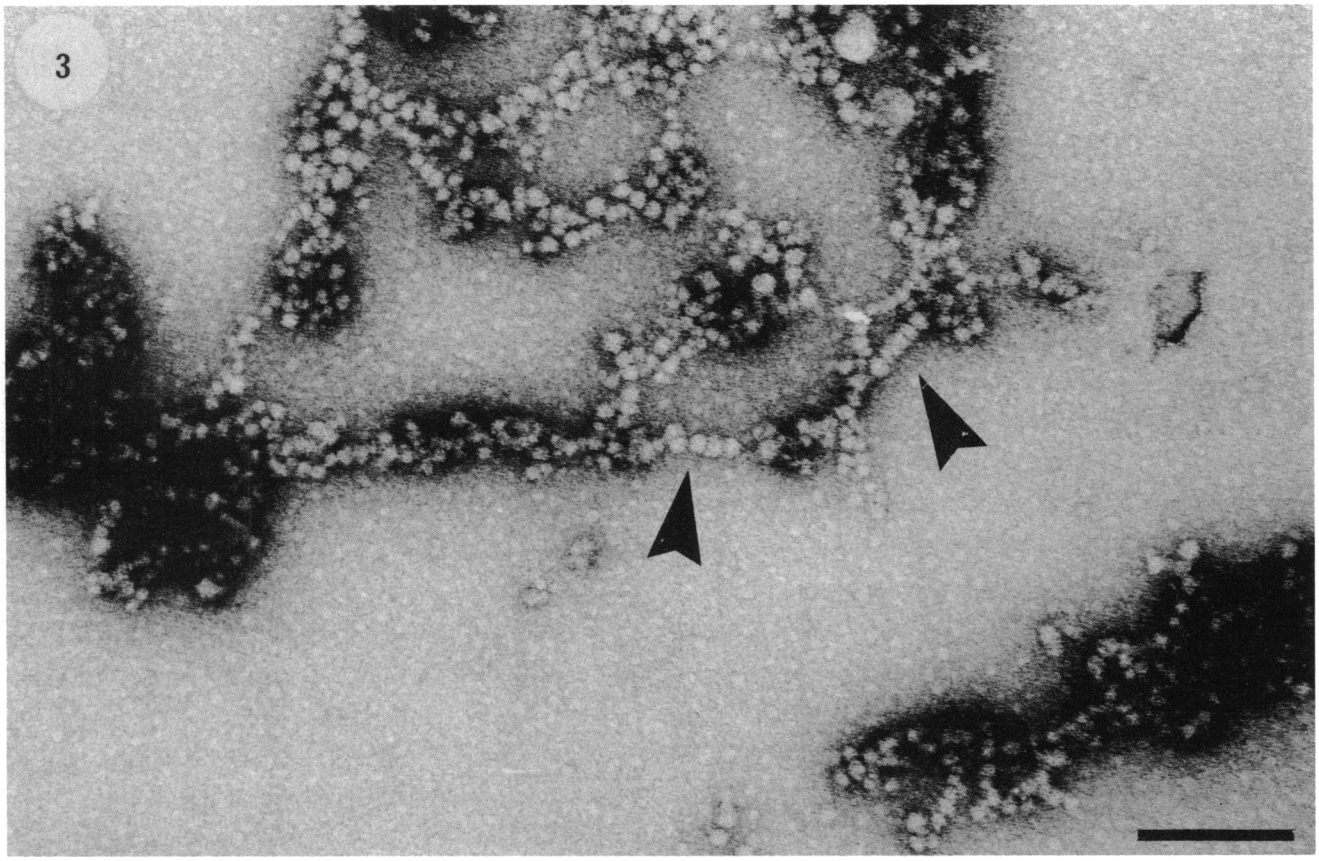

FIG. 3. Negative stain (2% uranyl acetate) of the PS sheath fraction dialyzed against 2% SDS. Note the linear arrangement of some of these assembly products (arrowheads). Most of the assembly products appear to be spheres of ca. 25 nm in diameter. Bar, 200 nm.

Markwell et al. (14). Bovine serum albumin (Sigma Chemical Co.) was used as a standard.

SDS-PAGE. Purified sheath and PI were solubilized by using SDS-polyacrylamide gel electrophoresis (PAGE) dissolution buffer (SDS–β-ME–EDTA at 100°C for 2 h [20]). PS was incubated for 5 min at 100°C in SDS-PAGE dissolution buffer. A Protean-II Mini-Gel System (Bio-Rad Laboratories, Richmond, Calif.) was routinely used to run SDS-PAGE by the method of Laemmli (13) with a 15% resolving gel described previously (20).

Glycoprotein staining. SDS-PAGE gels containing the solubilized sheath preparations were examined for the presence of glycoproteins by using the periodic acid-Schiff staining method described by Fairbanks et al. (8). Bovine A-1 glycoprotein (Sigma Chemical Co.) was used as a positive control for glycoprotein staining.

Production and selection of hybridomas. The method for production of monoclonal antibodies (MAbs) toward the sheath of *M. hungatei* GP1 has been previously described in detail (20) and was used in this study. Purified sheath was used as the antigen for the production and selection of MAbs.

Western immunoblotting. PS and PI fractions were studied by Western immunoblotting (6, 26) with MAbs from culture supernatants (20).

Electron microscopy. Samples were negatively stained with 2% (wt/vol) uranyl acetate on Formvar carbon-coated grids. These preparations were examined by transmission electron microscopy with a Philips EM300 electron microscope operating under standard conditions (60 kV) with the cold finger in place. Preparation of material for thin sectioning has been described previously (20).

Colloidal-gold labeling. Pure sheath was labeled first with PS fraction-specific MAbs and second with protein A (Boehringer Mannheim, Dorval, Quebec, Canada)-colloidal gold (1, 9, 10) as described previously (20). These immunogold-labeled preparations were examined as negative stains and in thin section by electron microscopy.

Surface localization of the PS fraction. Sheath (2 ml; 6 mg/ml) was combined with 200 μl of polycationized ferritin (PCF) (5.5 mg/ml) (Sigma Chemical Co.) and incubated at room temperature. Unassociated PCF was separated from the PCF-sheath by centrifugation (14,000 × *g* for 1 min) of the sheath. The PCF-sheath pellet was then washed through three 1-ml portions of dH_2O and finally resuspended into 1 ml of dH_2O. Glutaraldehyde (2% aqueous solution) fixation was required to examine the PCF-sheath by negative staining and in thin section. In a separate experiment, a 0.5-ml portion of the labeled sheath was made 90% (wt/vol) by addition to 4.5 g of solid phenol and reacted overnight at room temperature, separated into PS and PI fractions (as described before), and examined by SDS-PAGE. To prevent artificial (covalent) bonding between the PCF and the sheath, PCF-sheath was not fixed with glutaraldehyde prior to extraction of the PS fraction. A portion of the PI fraction produced from PCF-sheath was examined by transmission electron microscopy of negatively stained material and in thin section of standard embedded material.

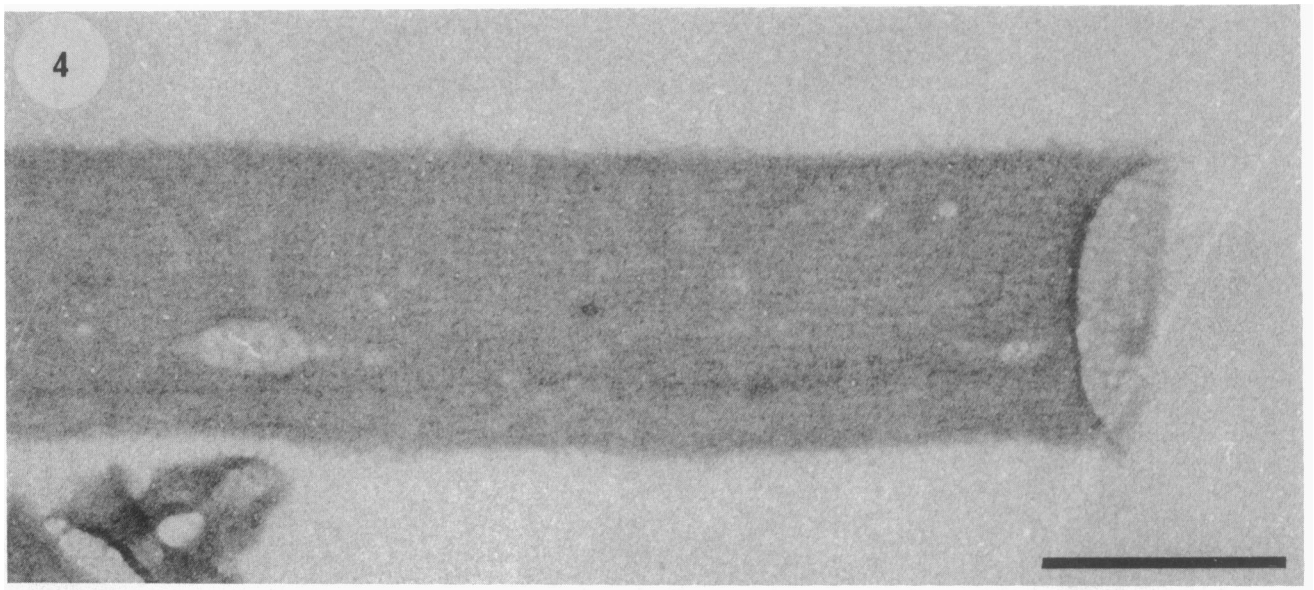

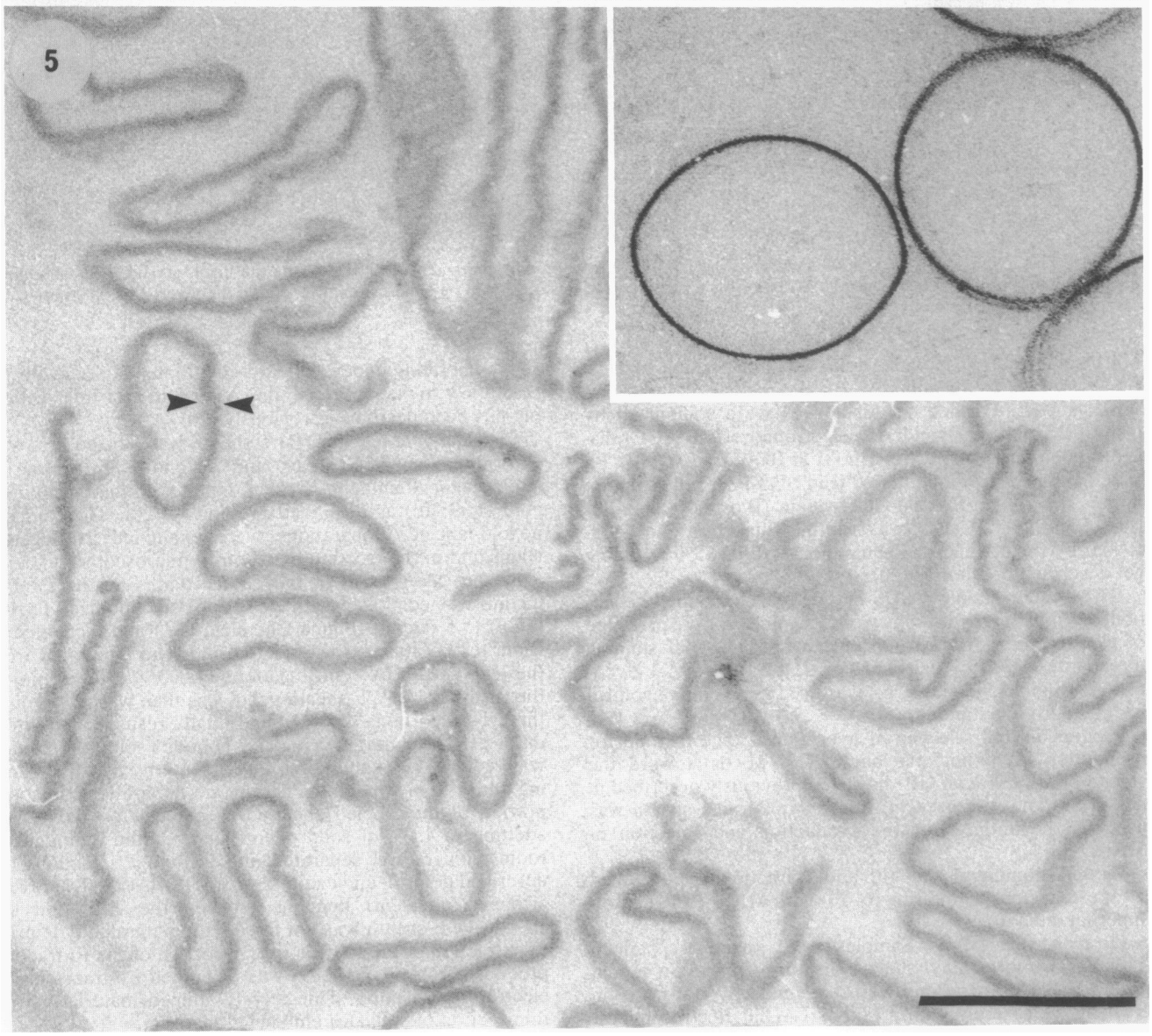

FIG. 4. Electron micrograph of the PI sheath fraction negatively stained with 2% uranyl acetate. Note the cross-hatched pattern on the sheath, which probably corresponds to the hoop boundaries and a previously unseen periodicity along the length of the sheath tubes (not evident in negative stains of intact sheath [Fig. 1]). Bar, 0.5 μm.

FIG. 5. Thin section of the PI sheath material dialyzed against 2% SDS and washed by centrifugation into dH_2O. Note the collapse of the sheath tubes and an increase in sheath thickness (arrowheads) as compared with untreated sheath (inset). Bar, 0.5 μm.

RESULTS

The sheath was not solubilized by incubation in dH_2O at 100°C for 48 h. However, in this preparation a longitudinal fracture was frequently observed on negatively stained sheath (Fig. 1) which was not obvious on untreated sheath (data not shown). Figure 1 demonstrates the resilience of the sheath to denaturation and serves as a control for the crystalline structure of the sheath.

We have previously shown (20) that 74% of the sheath (by mass) can be solubilized by its treatment with SDS–β-ME–EDTA at 100°C for 2 h (Fig. 2, lane 2). Treatment of sheath for 18 h with 90% phenol solubilized an additional 19% of the sheath (Fig. 2, lane 3). The PS fraction consists of two polypeptides, ca. 62 and 66 kDa, not seen in the SDS–β-ME–EDTA-solubilized sheath fraction. The PI fraction was indistinguishable from SDS–β-ME–EDTA-treated pure sheath (Fig. 2, lane 4).

Dialysis of the PS fraction into dH_2O resulted in a single large assembly product (of millimeter dimensions) with a plasticlike physical consistency. SDS-PAGE examination of this dialyzed product did not reveal any resolubilized sheath polypeptides. Thin sections revealed large (several micrometers) spherical assemblies all annealed into a macroscopic structure which did not possess periodic structure (data not shown). Dialysis of the PS fraction into 2% SDS resulted in the assembly of fine spheres ca. 25 nm in diameter (Fig. 3). These reassembled products possessed a preferred polarity, evident in the linear arrangement of the spheres.

The PI fraction could not be resuspended in dH_2O. However, continued mixing in the presence of 2% SDS resulted in the suspension of individual sheathlike structures, which could then be dispersed into dH_2O for negative staining (Fig. 4). These sheathlike structures were approximately three-quarters the diameter of intact sheath (cf. Fig. 1 and 4). Although hoop boundaries could be discerned on the PI sheath structures, the 2.8-nm periodicity characteristic of the outer face of intact sheath was not evident. Of interest, the PI material did not possess the minute 2.8-nm longitudinal striations seen in intact sheath, which may be a visible

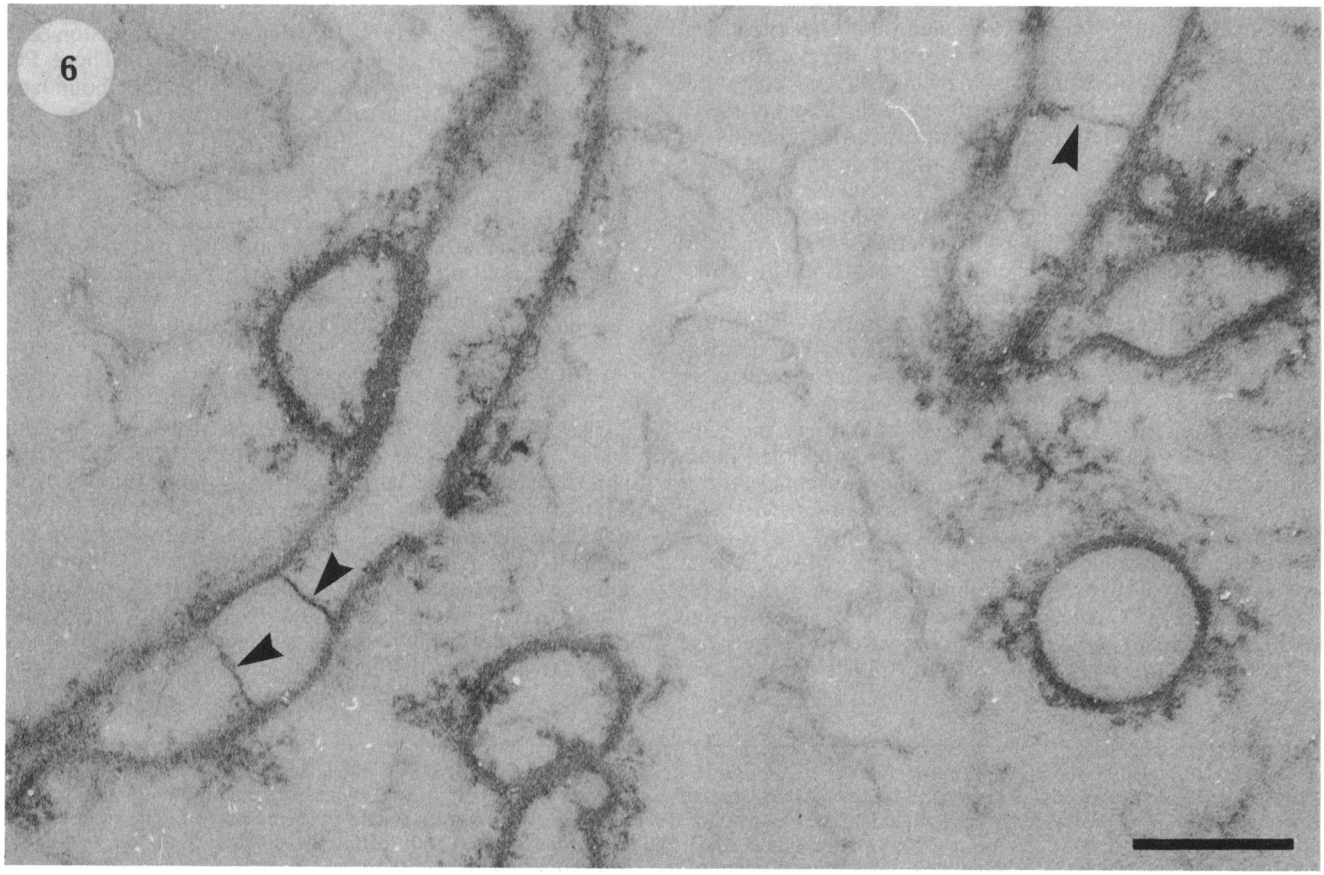

FIG. 6. Thin section of the PI fraction recombined with the PS fraction and dialyzed against 2% SDS. Note the aggregates on both the inner and outer surfaces of the sheath and the possible occurrence of cross walls (arrowheads). These reassembly products are more cylindrical than the PI sheath fraction (Fig. 4). Bar, 0.5 μm.

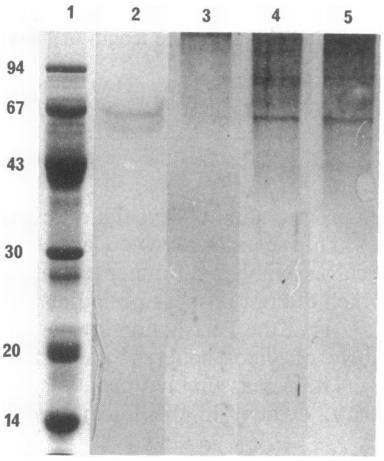

FIG. 7. Western immunoblot of PS sheath components (lane 2 stained with Coomassie brilliant blue R-250) probed with MAbs 1.8 (lane 3), 19.1 (lane 4), and 20.7 (lane 5). These MAbs demonstrated specificity toward the PS polypeptides and did not react with the SDS–β-ME–EDTA-soluble sheath fraction (data not shown). This provides immunochemical evidence for a distinct group of proteins (associated with the sheath of *M. hungatei* GP1). Lane 1 contains a Bio-Rad low-molecular weight standard stained with Coomassie brilliant blue R-250.

sign of the removal of PS polypeptides from the sheath. However, a faint broader longitudinal pattern which had not been seen before could be discerned. Examination of thin sections of the PI fraction revealed that the cylindrical shape, characteristic of untreated sheath, did not exist but was replaced by deformed, and in many cases collapsed, sheath tubes (Fig. 5). In thin section, the thickness of the PI fraction had increased in comparison with the thickness of untreated sheath. Presumably, the altered dimensions of the phenol-treated sheath corresponded to a release and a rearrangement of sheath polypeptides. SDS–β-ME–EDTA treatment, known to produce hoops from intact sheath, produced generally amorphous debris and only a few hooplike structures from the PI fraction (data not shown).

An attempt to reassemble bona fide sheath by combining the PI fraction in dH_2O with the undialyzed PS fraction was unsuccessful. Although 2.8-nm paracrystalline repeats were not produced, several intriguing observations were made. Cross-sections and longitudinal sections through the reassembled "product" (Fig. 6) more closely resembled intact sheath (cylindrical shape) than did the pleiomorphic PI forms previously seen (Fig. 5). The reassembled product also contained cross walls in longitudinal sections.

Western immunoblot analysis showed that MAb 1.8 demonstrated reactivity towards an upper range (>67 kDa) of the PS fraction (Fig. 7, lane 3) whereas MAbs 19.1 (lane 4) and 20.7 (lane 5) demonstrated reactivity toward the entire range of PS polypeptides. Reactivity of MAb 1.8 may be restricted to an epitope resulting from the association of more than one PS polypeptide. Western immunoblot analysis of the PI fraction by using the anti-PS polypeptide MAbs demonstrated that low levels of PS proteins were still associated with the PI fraction (data not shown). These MAbs did not react with SDS–β-ME–EDTA-treated sheath subjected to Western immunoblot analysis.

Our next goal was to identify whether the PS polypeptides could be localized on the inner or outer faces of the sheath by using immunogold probes. Control experiments for nonspecific binding of colloidal gold, antibody probes (Fig. 8B), and protein A-colloidal gold alone gave negative results. Used in conjunction with protein A-colloidal gold, proteins reactive with MAbs 1.8, 19.1, and 20.7 were localized to linear regions along the longitudinal axis of the sheath (Fig. 8A). Those for MAbs 1.8 and 19.1 were also located at transverse regions along the sheath and at one end of the sheath tube. The linear labeling pattern was observed primarily along the external surface of the sheath (Fig. 9A), whereas the transverse labeling pattern was observed on the internal surface of the sheath (Fig. 9B). Random sites were also recognized when MAb 19.1 was used. Protein A-colloidal gold immunolabeling of the PI fraction with MAb 19.1 (specific for the PS fraction) also demonstrated that PS peptides were still associated with the residual sheath structures (data not shown). However, the degree of labeling was greatly reduced (by more than 90%) when compared with the degree of colloidal-gold labeling present on untreated sheath.

The relationship between the PS polypeptides and the 2.8-nm paracrystalline repeat on the outer face of the sheath was studied by using a PCF probe. Purified sheath bound the PCF on its outer face (Fig. 10), almost to the exclusion of the inner face (shown in thin section [Fig. 11]). These PCF macromolecules were also aligned with the hoop boundaries (Fig. 12). Examination of the PI fraction produced from PCF-labeled sheath demonstrated the retention of the PCF in this fraction (Fig. 13). The poor negative staining of the ferritin macromolecules may have been due in part to the poor wettability of PI material, but was more probably due to the dispersal of PCF throughout the thickness of the sheath (visualized in thin sections [Fig. 14]). Even though PCF was distributed throughout the thickness in PI, a weak orientation of PCF with the hoops was still evident.

DISCUSSION

The sheath of *M. hungatei* GP1 is a resilient, proteinaceous, paracrystalline bilayer structure (3, 5, 21, 24). Its ability to withstand various dissolution conditions (5) has been attributed to the presence of strategic disulfide bonds (20, 21). The function of the sheath as a physical barrier is implied by this resilience and also by the ability of the filaments to exclude the crystal violet of the Gram stain (4). The sheath is also a rigid structure (cylinder), presumably because of covalent bonding in combination with weaker bonds (e.g., ionic bonding and hydrophobicity). Rigidity in

FIG. 8. (A) Negative stain (2% uranyl acetate) of *M. hungatei* GP1 sheath probed with MAb 19.1 and labeled with protein A-colloidal gold. Note the presence of colloidal gold along the length of the sheath tube at several transverse sites (arrowheads) and at other diffuse sites. This labeling pattern provides evidence for limited surface exposure of the PS proteins. (B) Negative stain of sheath probed with MAb 19.1 and colloidal gold. The low levels of labeling with colloidal gold evident in these micrographs give us confidence in our method of antibody-mediated protein A-colloidal gold surface localization of the PS sheath proteins. Bar, 0.5 μm.

FIG. 9. Thin section of purified sheath labeled with MAb 19.1 and protein A-colloidal gold. Analysis of thin sections demonstrated the surface exposure of PS proteins in the longitudinal, linear arrangement (Fig. 8) on the outer face of the sheath (A) and in the transverse, linear arrangement (Fig. 8) on the inner face of the sheath (B). Bar, 0.5 μm.

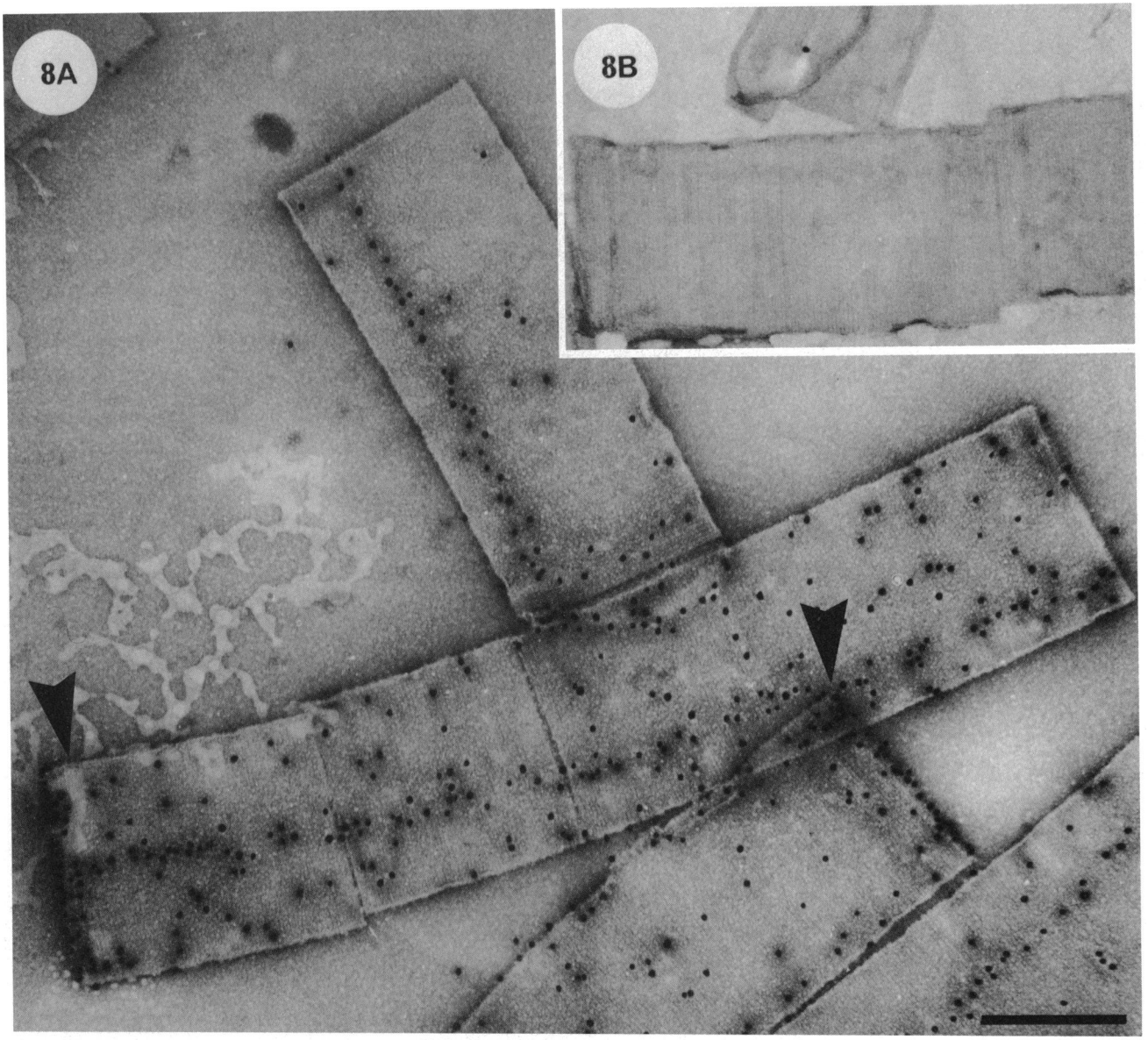

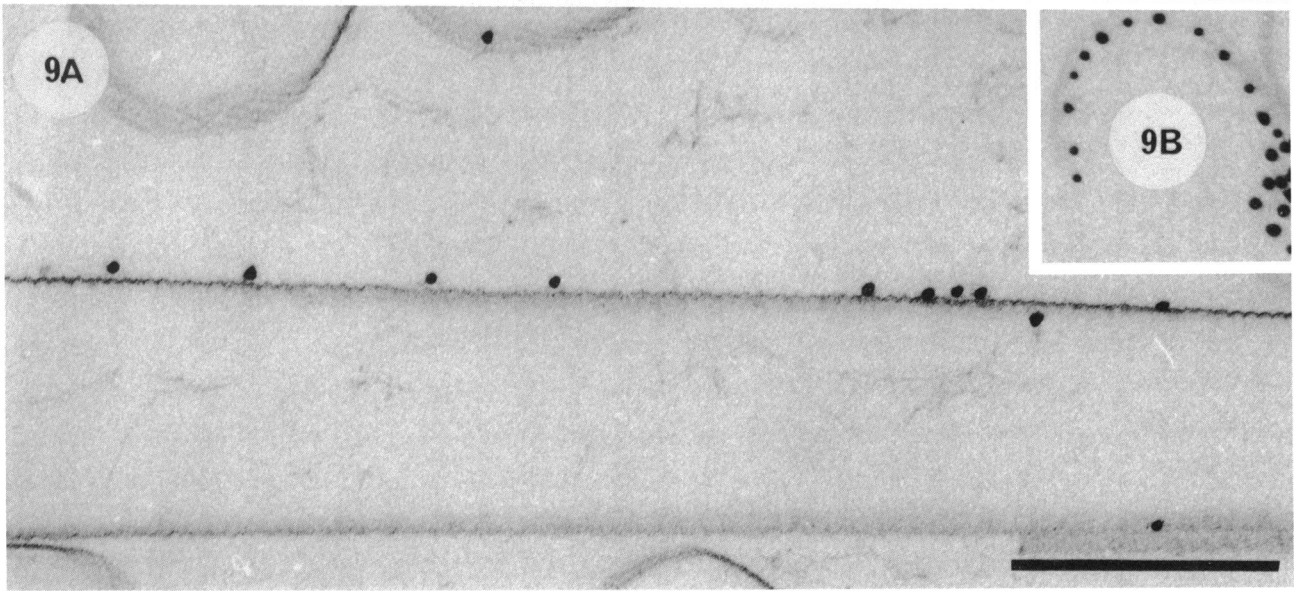

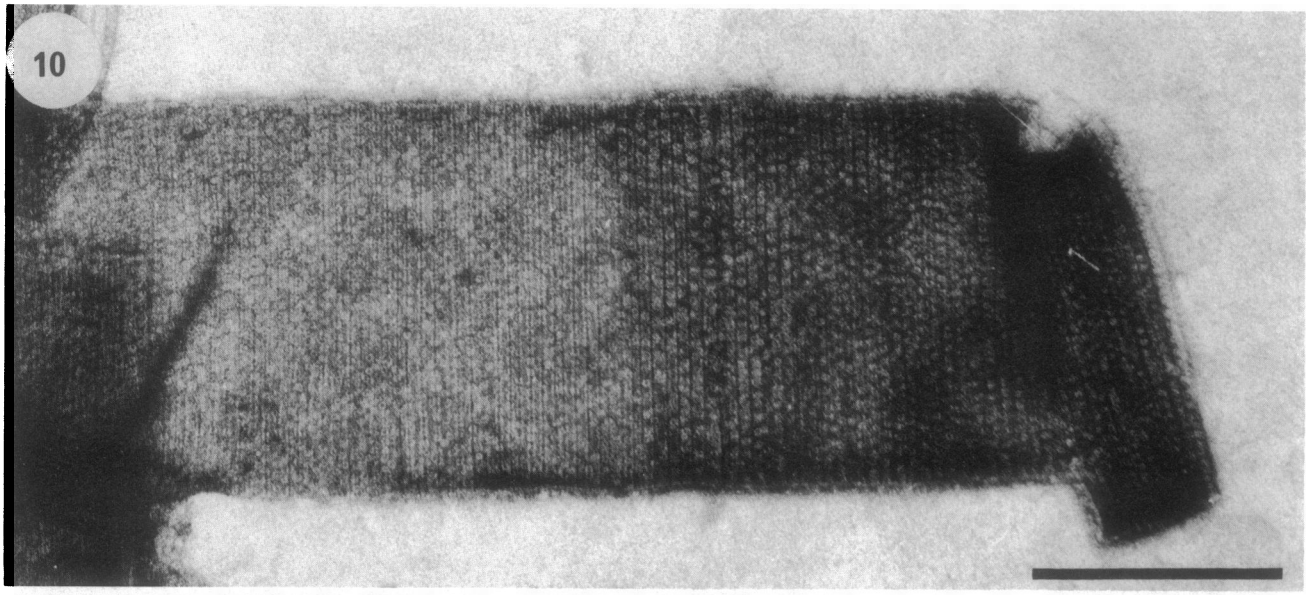

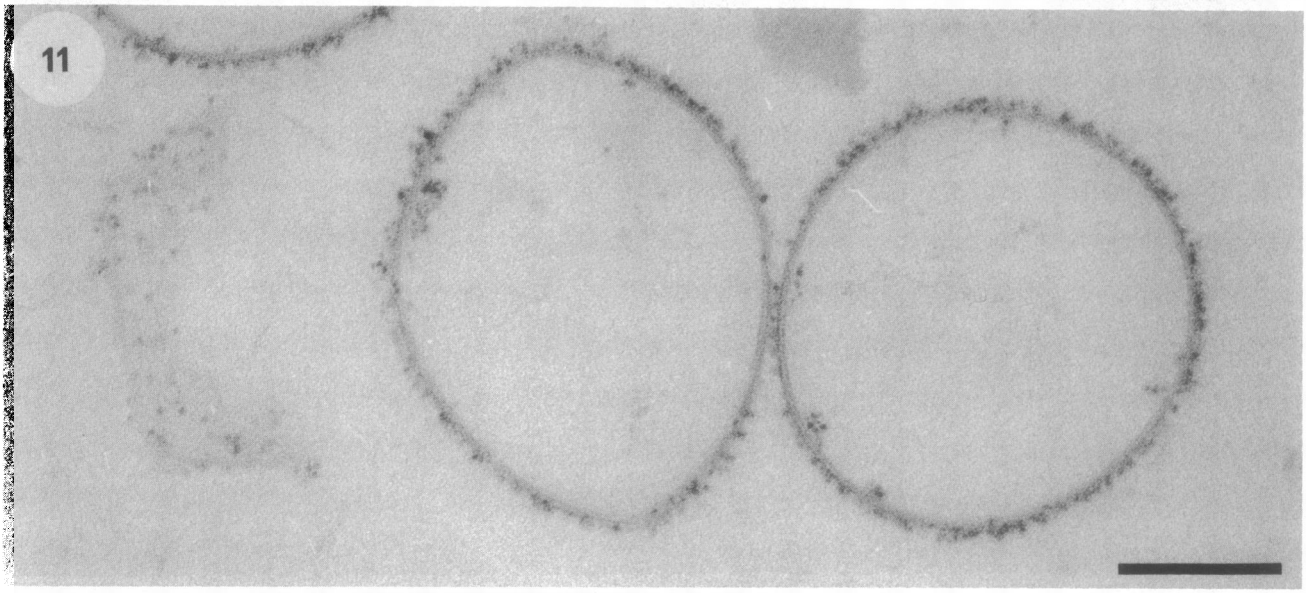

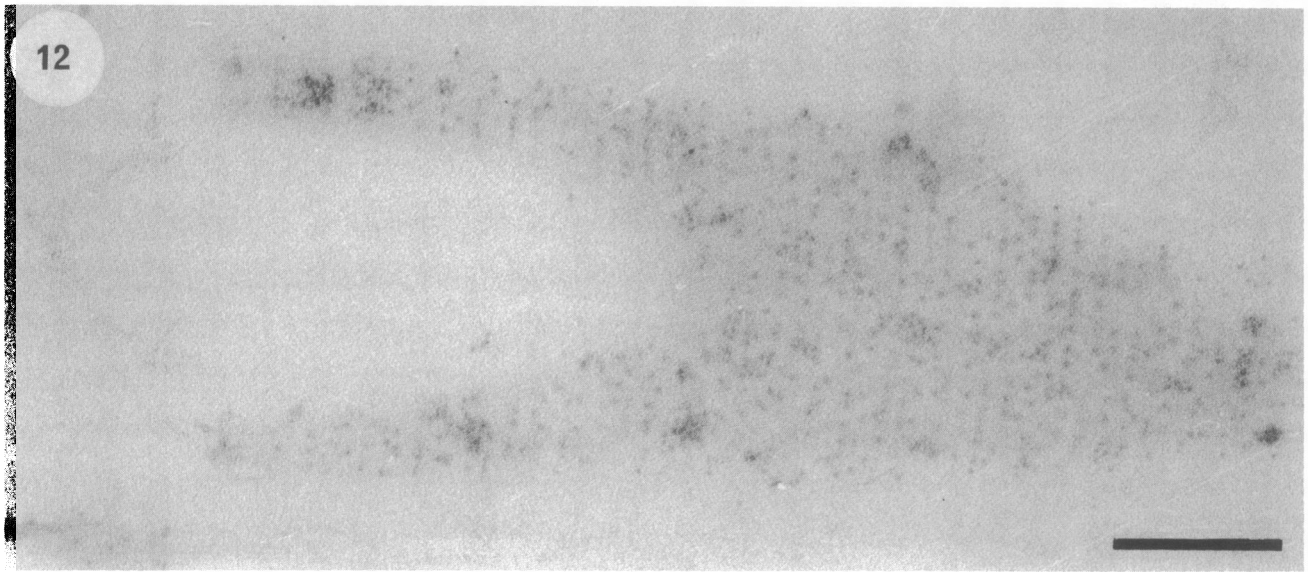

FIG. 10. Negative stain (2% uranyl acetate) of sheath probed with PCF and fixed with glutaraldehyde. Note the linear labeling pattern of the PCF (donut shaped with electron dense centres) along the hoop structures. Bar, 0.5 μm.

FIG. 11. Thin section of purified *M. hungatei* GP1 sheath probed with PCF. The ferritin is localized primarily onto the external surface of the sheath. Bar, 200 nm.

FIG. 12. Thin section of purified *M. hungatei* GP1 sheath probed with PCF. The ferritin is aligned along the hoop axis. Bar, 200 nm.

conjunction with the 2.8-nm surface repeat (24) should allow the sheath to function as a molecular sieve.

The original model for the sheath of *M. hungatei* consisted of an outer layer composed of 24-kDa polypeptides and of an inner layer composed of high-molecular-mass ($>10^3$ kDa) proteinaceous material (21). Recently, we (20) modified this bilayer model by using an SDS–β-ME–EDTA dissolution technique which solubilized 74% of the sheath (by mass) in a range of polypeptides from 10 to 40 kDa. These polypeptides were localized to either the inner or outer face of the sheath (MAb probe dependent), which suggested that the sheath was a bilayer structure composed of polypeptides assembled in a specific, inner-outer orientation to the bacterial surface. The existence of lower-range polypeptides (10 to ca. 30 kDa) was attributed to the extremely harsh dissolution process (described in Materials and Methods of reference 20). This was substantiated by their limited reactivity with MAbs directed toward the sheath (20). Since β-ME, a disulfide bond breaker, was required for the solubilization of these polypeptides, the SDS–β-ME–EDTA polypeptides were implicated in the resilience of the sheath through intersubunit disulfide bonding (20).

In the present study we have isolated a novel, PS group of polypeptides from the sheath of *M. hungatei* GP1. This PS fraction was composed of predominantly 62- and 66-kDa polypeptides and represented 19% of the sheath (by mass). This represents our second modification of the original model described by Sprott et al. (21) in that there are now two groups of proteins which can be solubilized from pure sheath (Fig. 2).

Isolation of PS polypeptides from the sheath caused drastic structural changes to the sheath, with its loss of surface periodicity (Fig. 4) and cylindrical integrity (Fig. 5). The PI fraction differed markedly from the SDS–β-ME–EDTA-resistant hoops (20) which possessed the 2.8-nm surface repeat and the rigidity of the sheath. In the PI fraction, the periodicity loss can be attributed to a solvent effect. Phenol denatures proteins to their primary structure without cleavage of covalent bonds (25) and normally results in a more loosely folded molecule. It is probable that the sheath would take on a more fuzzy or loosely packed appearance after phenol treatment. At the same time, noncovalently bound polypeptides would be released. Removal of the phenol would result in the collapse of these extended polypeptides, perhaps trapping PS proteins. The production of pliable sheathlike structures (PI polypeptides) which did not possess the cylindrical form characteristic of pure sheath (Fig. 5) suggests a role for the PS fraction in sheath rigidity. Subsequent recombination of PS and PI fraction restored the apparent rigidity of the sheath (i.e., the cylindrical form [Fig. 6]), although bona fide sheath structures were not produced. We do not know the placement of PS in these reassembly forms.

In addition to a role in sheath rigidity, the PS fraction may play a role in sheath resilience. In Western immunoblotting, PS fraction-specific MAbs did not label any polypeptides released from pure sheath by SDS–β-ME–EDTA treatment. This suggests a role for the PS fraction in the resilience of the insoluble hoops remaining after SDS–β-ME–EDTA treatment (20). The inability to detect PS polypeptides in this soluble fraction may relate to their amounts (sensitivity of our immunoassay) or to their stability during the prolonged incubation (2 h) at 100°C.

By labeling the 2.8-nm surface repeat of the sheath with PCF (Fig. 10 to 12) and extracting the PS fraction without its removal (Fig. 13 and 14), we determined that the PS fraction does not contribute directly to the 2.8-nm paracrystalline repeat. Therefore, the paracrystalline structure evident in intact sheath must be conferred by the SDS–β-ME–EDTA-soluble polypeptides. These surface polypeptides were also localized to the inner surface of the sheath (20). A coordinated assembly of the molecular components (SDS–β-ME–EDTA soluble and PS fraction) of the sheath must be used to maintain such a highly ordered structure. Therefore, we can speculate that, like the SDS–β-ME–EDTA-soluble polypeptides, the PS polypeptides also occur in a specific orientation in relation to the bacterial surface. A preferred, ordered arrangement of PS polypeptides within pure sheath is also implied by the linear orientation of the SDS-dialyzed PS reassembly products (chains of 25-nm spheres [Fig. 3]). On intact sheath, limited surface exposure of the PS fraction (Fig. 8A) suggests that these polypeptides reside within the framework of the sheath (consisting of SDS–β-ME–EDTA-soluble polypeptides).

M. hungatei grows at two distinct levels, first at the cell level by cell growth and division and second at the filament level by sheath splitting (2). The mechanism(s) of sheath growth and extension during these processes is unknown. Certainly, growth of *M. hungatei* sheath must be a highly coordinated process to assemble two groups of polypeptides into a crystalline lattice. To accommodate growth, sheath precursors must be able to integrate with the existing surface macromolecules. Lattice faults in the 2.8-nm repeat have been described as possible growth sites of sheath (18). Of interest, surface exposure of the PS polypeptides occurred in two unique arrangements: first in a linear, longitudinal pattern on the outer face on the sheath (Fig. 9A) and second in a linear, transverse pattern on the inner face on the sheath (Fig. 9B). This surface exposure of PS (sheath) polypeptides (Fig. 8 and 9) provides two possible lattice defects which can be related to sheath growth. If the longitudinal, linear PS domain represents a growth region, sheath growth would occur along the entire length of the cylinder, probably as a sliding fault which moves around the circumference of the sheath in a linear, coordinated manner. Incorporation of new sheath material would result in an overall increase in the length of the sheath and would correspond to cell growth. The second growth process, filament division, might then be represented by the transverse PS domains which occur primarily at the ends of sheath tubes. It is not known whether sheath growth occurs throughout the length of the sheath cylinder or whether it is restricted to active growth zones (i.e., sites of cell division), as determined for the S-layer polypeptides in *Bacillus sphaericus* (11).

In addition to sheath growth, the sheath should undergo some sort of maturation or turnover of its constituents. The

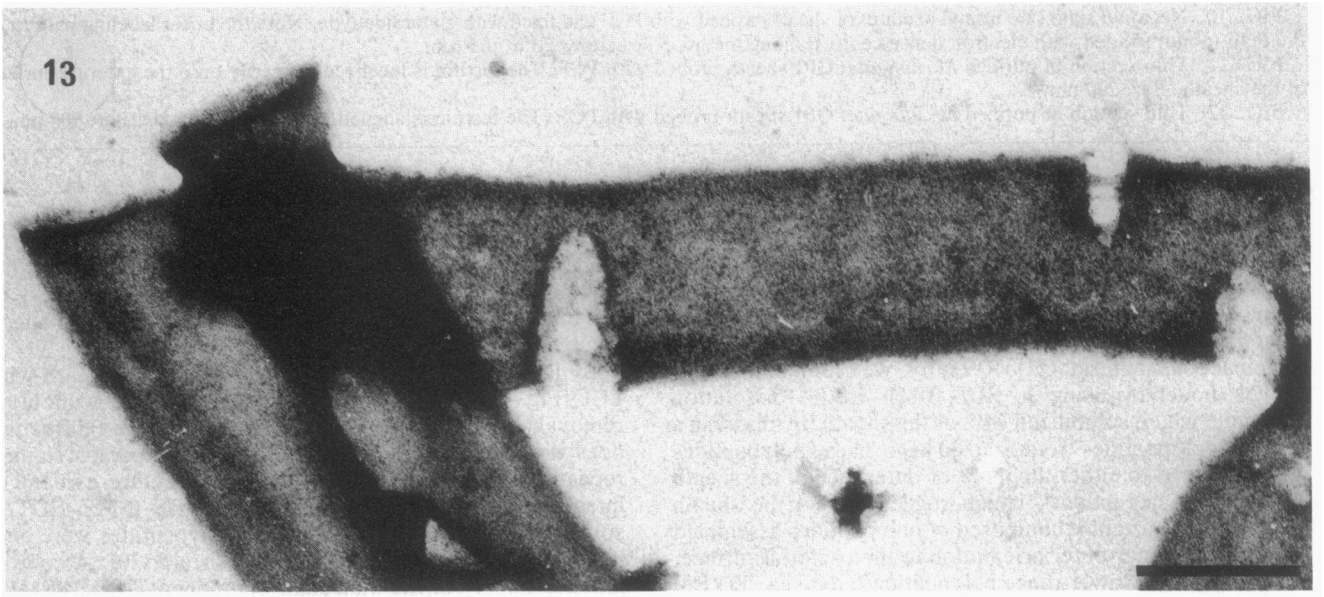

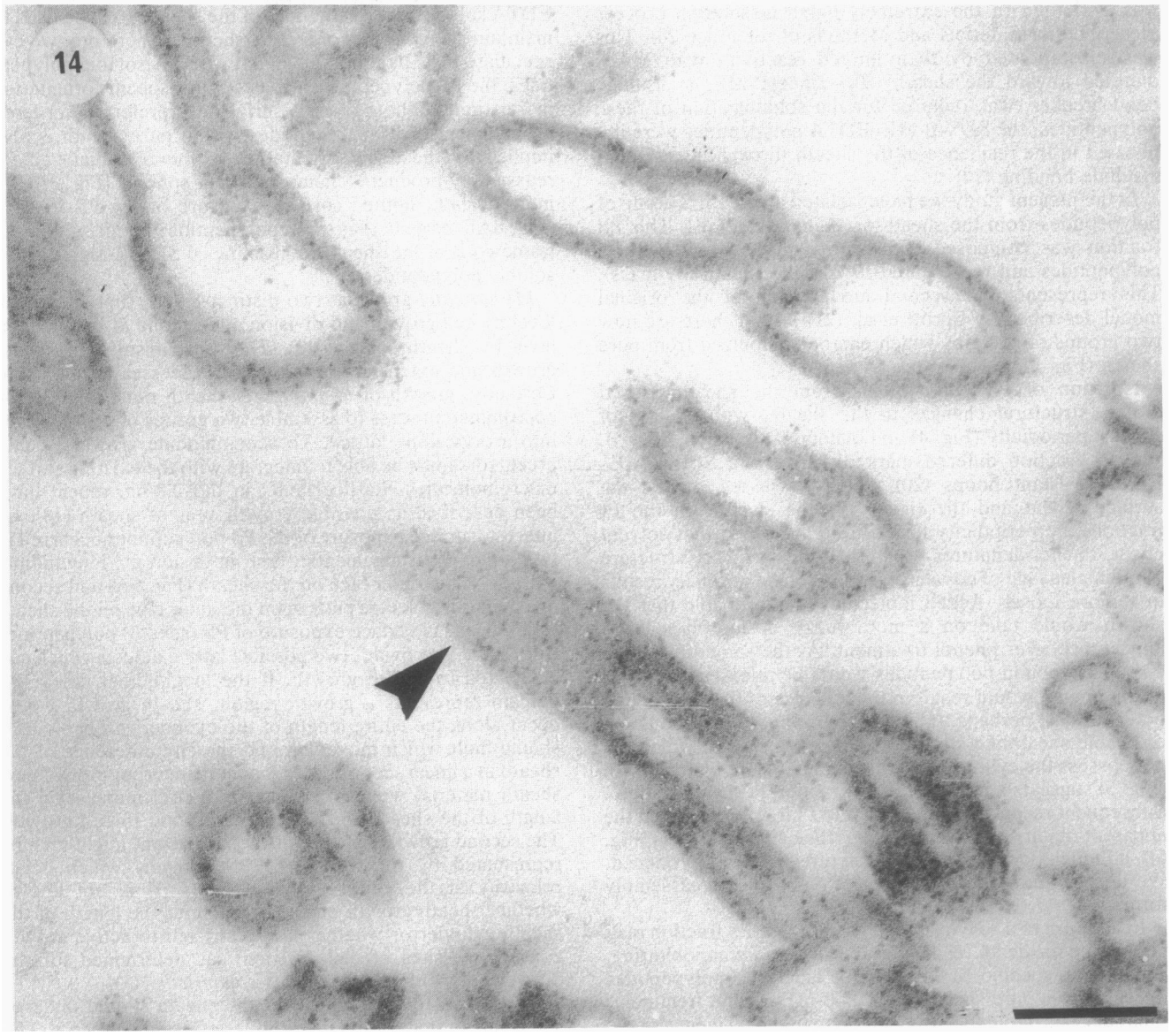

FIG. 13. Negative stain of the PI sheath fraction prepared by using PCF-labeled sheath. Note the electron-dense particles, which correspond to the PCF molecules. Removal of the PS proteins from PCF-sheath preparations without the removal of the PCF suggests that the SDS–β-ME–EDTA-solubilized proteins are responsible for the 2.8-nm periodicity on the outer face of the sheath (to which the PCF was bound [Fig. 11]). Bar, 0.5 μm.

FIG. 14. Thin section of the PI fraction prepared from the PCF-labeled sheath. Note the linear arrangement of the ferritin along the hoop axis (arrowhead) and the presence of the ferritin throughout the thickness of the PI sheath material. Distribution of the PCF throughout the sheath suggests that the phenol treatment denatures the sheath in such a way that reassembly of de novo sheath (by removal of the phenol) is unlikely (Fig. 6). Bar, 200 nm.

sheath possesses similar polypeptides on both its inner and outer faces (20) but restricts the 2.8-nm repeat to the outer face. Therefore, the paracrystalline repeat on the outer face of the sheath of *M. hungatei* may reflect a maturation or stress-releasing process occurring during sheath growth. In this context, we could imagine that the outer face possesses an easily defined lattice because at this elevation in the sheath fabric there is less covalent bonding. Since the outer face has a slightly larger circumference than the inner face, the units which make up the 2.8-nm lattice may be more widely separated here. This would be the stress-releasing event in which a migration of sheath protein from the inner to the outer face (new material to old material, respectively) would be required. The resilience imparted by the PS polypeptides to the sheath structure may reflect the stress-bearing region of the sheath in which maturation (release of stress) would then correspond to dissociation of PS polypeptides (from the SDS–β-ME–EDTA polypeptides) at the outer face of the sheath.

The work described in this paper now makes the sheath of *M. hungatei* more complex. In addition to the SDS–β-ME–EDTA-soluble polypeptides, which convey resilience to the sheath (20), a second group of polypeptides (PS polypeptides), which convey rigidity and probably resilience to the sheath, must now be incorporated into this proteinaceous bilayer structure (3, 5, 21). At the molecular level we propose a trilaminar structure involving an SDS–β-ME–EDTA—PS—SDS–β-ME–EDTA format. The high integrity and complexity of intact sheath (i.e., few lattice faults) makes growth difficult to model, although PS surface domains may represent insertion sites for sheath precursors, and suggests that sheath growth occurs throughout its length.

ACKNOWLEDGMENTS

G.S. was supported by a Natural Sciences and Engineering Research Council of Canada Graduate Student Fellowship during this study. The actual research was supported by an operating grant from the Medical Research Council of Canada to T.J.B.

The assistance of G. D. Sprott, Division of Biological Sciences, National Research Council of Canada, in growing large quantities of *M. hungatei* is greatly appreciated. Special thanks to C. MacKenzie for word processing.

REFERENCES

1. **Bendayan, M.** 1982. Double immunocytochemical labelling applying the protein A-gold technique. J. Histochem. Cytochem. **30**:81–85.
2. **Beveridge, T. J., B. J. Harris, and G. D. Sprott.** 1987. Septation and filament splitting in *Methanospirillum hungatei*. Can. J. Microbiol. **33**:725–732.
3. **Beveridge, T. J., G. Southam, M. H. Jericho, and B. L. Blackford.** 1990. High resolution topography of the S-layer sheath of the archaebacterium *Methanospirillum hungatei* provided by scanning tunneling microscopy. J. Bacteriol. **172**:6589–6595.
4. **Beveridge, T. J., G. D. Sprott, and P. Whippey.** 1991. Ultrastructure, inferred porosity, and Gram-staining character of *Methanospirillum hungatei* filament termini describe a unique cell permeability for this archaeobacterium. J. Bacteriol. **173**: 130–140.
5. **Beveridge, T. J., M. Stewart, R. J. Doyle, and G. D. Sprott.** 1985. Unusual stability of the *Methanospirillum hungatei* sheath. J. Bacteriol. **162**:728–737.
6. **Burnette, W. N.** 1981. "Western blotting": electrophoretic transfer of proteins from sodium dodecyl sulfate-polyacrylamide gels to unmodified nitrocellulose and radiographic detection with antibody and radioiodinated protein A. Anal. Biochem. **112**:195–203.
7. **Conway de Macario, E., H. König, and A. J. L. Macario.** 1986. Antigenic determinants distinctive of *Methanospirillum hungatei* and *Methanogenium cariaci* identified by monoclonal antibodies. Arch. Microbiol. **144**:20–24.
8. **Fairbanks, G., T. L. Steck, and D. F. H. Wallach.** 1971. Electrophoretic analysis of the major polypeptides of the human erythrocyte membrane. Biochemistry **10**:2606–2617.
9. **Frens, G.** 1973. Controlled nucleation for the regulation of the particle size in monodisperse gold suspensions. Nature (London) **241**:20–22.
10. **Hicks, D., and R. S. Molday.** 1984. Analysis of cell labelling for scanning and transmission electron microscopy, p. 203–219. *In* J. P. Revel, T. Barnard, and G. H. Haggis (ed.), The science of biological specimen preparation for microscopy and microanalysis. SEM Inc., Chicago.
11. **Howard, L. V., D. D. Dalton, and W. K. McCourbrey.** 1982. Expansion of the tetragonally arrayed cell wall protein layer during growth of *Bacillus sphaericus*. J. Bacteriol. **149**:748–757.
12. **Koval, S. F., and R. G. E. Murray.** 1984. Isolation of surface array proteins from bacteria. Can. J. Microbiol. **62**:1181–1189.
13. **Laemmli, U. K.** 1970. Cleavage of structural proteins during the assembly of the head of bacteriophage T4. Nature (London) **227**:680–685.
14. **Markwell, M. A., S. M. Haas, L. L. Breter, and N. E. Tolbert.** 1978. A modification of the Lowry procedure to simplify protein determination in membrane and lipoprotein samples. Anal. Biochem. **87**:206–210.
15. **Patel, G. B., L. A. Roth, and G. D. Sprott.** 1979. Factors influencing filament length of *Methanospirillum hungatii*. J. Gen. Microbiol. **112**:411–415.
16. **Patel, G. B., L. A. Roth, L. van den Berg, and D. S. Clark.** 1976. Characterization of a strain of *Methanospirillum hungatii*. Can. J. Microbiol. **22**:1404–1410.
17. **Patel, G. B., G. D. Sprott, R. W. Humphrey, and T. J. Beveridge.** 1986. Comparative analysis of the sheath structures of *Methanothrix concilii* GP6 and *Methanospirillum hungatei* strains GP1 and JF1. Can. J. Microbiol. **32**:623–631.
18. **Shaw, P. J., G. J. Hills, J. A. Henwood, J. E. Harris, and D. B. Archer.** 1985. Three-dimensional architecture of the cell sheath and septa of *Methanospirillum hungatei*. J. Bacteriol. **161**:750–757.
19. **Sleytr, U. B., and P. Messner.** 1988. Crystalline surface layers in prokaryotes. J. Bacteriol. **170**:2891–2897.
20. **Southam, G., and T. J. Beveridge.** 1991. Immunochemical analysis of the sheath of the archaeobacterium *Methanospirillum hungatei* strain GP1. J. Bacteriol. **173**:6213–6222.
21. **Sprott, G. D., T. J. Beveridge, G. B. Patel, and G. Ferrante.** 1986. Sheath disassembly in *Methanospirillum hungatei* strain GP1. Can. J. Microbiol. **32**:847–854.
22. **Sprott, G. D., J. R. Colvin, and R. C. McKellar.** 1979. Spheroplasts of *Methanospirillum hungatii* formed upon treatment with

dithiothreitol. Can. J. Microbiol. **25**:730–738.
23. **Sprott, G. D., and R. C. McKellar.** 1980. Composition and properties of the cell wall of *Methanospirillum hungatei*. Can. J. Microbiol. **26**:115–120.
24. **Stewart, M., T. J. Beveridge, and G. D. Sprott.** 1985. Crystalline order to high resolution in the sheath of *Methanospirillum hungatei*: a cross-beta structure. J. Mol. Biol. **183**:509–515.
25. **Thorun, W., and E. Mehl.** 1968. Determination of molecular weight of microgram quantities of protein components from biological membranes and other complex mixtures: gel electrophoresis across linear gradients of acrylamide. Biochim. Biophys. Acta **160**:132–134.
26. **Towbin, M., T. Staehlin, and J. Gordon.** 1979. Electrophoretic transfer of proteins from polyacrylamide gels to nitrocellulose sheets: procedure and some applications. Proc. Natl. Acad. Sci. USA **76**:4350–4354.